

Large N-Heteroacenes: New Tricks for Very Old Dogs?

Uwe H. F. Bunz,* Jens U. Engelhart, Benjamin D. Lindner, and Manuel Schaffroth

acenes · electron-transport materials · heteroacenes ·
polycyclic heteroarenes · nitrogen heterocycles

Dedicated to Prof. Klaus Müllen

Azaacenes have been known for a very long time, either as N,N' -dihydro compounds or in their oxidized form as $4n + 2\pi$ systems, but only recently have processable and characterizable derivatives been sought. In the last three years synthetic routes to large N-heteroacenes have been developed. In particular, the Pd-catalyzed coupling of aromatic diamines with activated aromatic dihalogenides has enabled simple access to numerous new azaacenes. Since 2010, azapentacene and stable oligoazahexacene have been synthesized, as well as a symmetrical tetraazapentacene, which acts as an excellent electron-transport material for thin-film transistors.

elements into the framework of the acenes. The substitution of CH units through nitrogen atoms to generate pyridine or pyrazine rings comes to mind. The resulting N-heteroacenes should display attractive properties,

1. Scope, Limitations, and Background

This Minireview details the recent developments in the field of large N-heteroacenes (since 2010) and their use in organic electronics. Around 5000 articles (September 2012) have been published on the topic of pentacene and its derivatives, because they (besides rubrene) are “the poster child” for sublimation-processable hole transporters in organic thin-film transistors. A favorable combination of structure and molecular packing results in hole mobilities for pentacene that reach up to $58 \text{ cm}^2 \text{ V}^{-1} \text{ s}^{-1}$ when working under cryogenic conditions.^[1] However, pentacene is for practical reasons an unfavorable electron-transporting material.^[2] One of the reasons for this is the high sensitivity of the formed pentacene radical anions, which lose their charge in trap states, or to adventitious traces of oxygen, which is difficult to exclude, even in encapsulated devices.

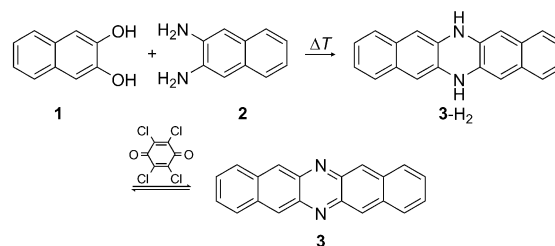
What would be necessary to “mutate” pentacene into a potent electron-transport material, that is, an n -channel semiconductor? One might take pentacene and lower both its HOMO as well as its LUMO, so that the radical anions formed upon charge injection (the delocalized charge carriers in the crystalline solid) would have energies that are below that of trap states, and also unable to reduce oxygen. A suitable way to do this could be by the electronegative substitution of either the hydrogen atom by halogen atoms or other acceptors^[3] or the introduction of electronegative

complementary to those of the “normal” acenes.

The last five years have witnessed significant activity in the synthesis and property evaluation of larger N-heteroacenes. Several overviews have already been written,^[4] but the area has expanded such that a new overview of this exciting and emerging topic is timely. It is important to look at issues that encompass synthetic approaches, structures, physical and optical properties, as well as applications of N-heteroacenes in organic electronic devices. Here we present developments since 2010.

2. Historical Overview

Pentacene was first synthesized in 1935 by Clar and John.^[5] The larger but reduced N-heteroacenes were, however, prepared by Hinsberg^[6] as well as Fischer and Hepp^[7] considerably earlier. They described the synthesis and properties of a series of N,N' -dihydrooligoazapentacenes such as **3-H₂** (Scheme 1). In the 1960s Kummer and Zimmermann^[8] and Leete et al.^[9] demonstrated that fluorescent **3-H₂** could be



Scheme 1. Synthesis of diazapentacene **3** via **3-H₂**.

[*] Prof. U. H. F. Bunz, Dipl.-Chem. J. U. Engelhart,
Dipl.-Chem. B. D. Lindner, M. Sc. M. Schaffroth
Organisch-Chemisches Institut, Ruprecht-Karls-Universität
Im Neuenheimer Feld 270, 69120 Heidelberg (Germany)
E-mail: uwe.bunz@oci.uni-heidelberg.de

oxidized into the diazapentacene **3**. Chloranil, copper(II), or lead(IV) salts effect the oxidation, but **3-H₂** very slowly oxidizes into **3** on exposure to air.

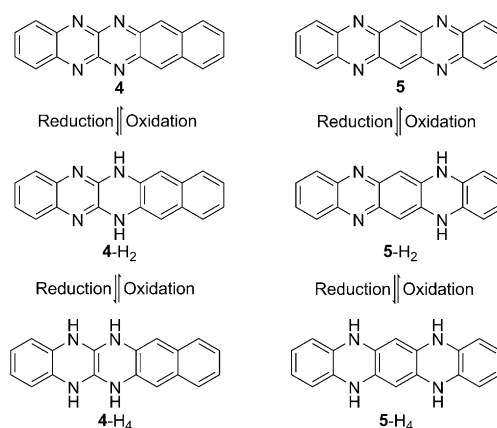
Similar oxidation reactions have made the tetraazaacenes **4** and **5** accessible from their respective *N,N'*-dihydrogenated precursors **4-H₂** and **5-H₂**. These azaacenes, however, were only characterized by their UV/Vis spectra. Later, Nuckolls and co-workers demonstrated that **3-H₂** is a suitable replacement for pentacene and functions as a *p*-transporting material with mobilities up to 0.30–0.45 cm² V⁻¹ s⁻¹.^[10]

3. Classification of *N*-heteroacenes and the Question of Their Aromaticity

An important aspect of the heteroacenes is their aromaticity.^[11] Diaza- and tetraazapentacenes occur both in their reduced as well as in their oxidized form. In a formal sense, the *N,N'*-dihydro compounds such as **3-H₂**, **4-H₂**, and **5-H₂** are antiaromatic. Nucleus-independent chemical shift (NICS) and thermochemical calculations, however, unveil a more complex picture.

The aromaticity of the *N,N'*-dihydroazaacenes is lower than that of the azaacenes, but they are stabilized, as the breakup of one large aromatic system into two smaller ones is, according to Clar's rule, advantageous. Further reduction to **4-H₄** or **5-H₄**, however, is not easily possible (Scheme 2), and **3-H₄**–**5-H₄** remain unknown. The *N,N'*-dihydroazaacenes, thus, rest in an energetic valley of stability.

An important question for molecules such as **4-H₂** and **5-H₂** is the position of the hydrogen substituents on the nitrogen



Scheme 2. Oxidation states of the tetraazaacenes **4** and **5**.

atoms, as both compounds could, in principle, exist in their quinone-type structure. However, NMR experiments and quantum chemical calculations demonstrate that the tautomers depicted are more stable than the alternatives.^[12]

According to Clar's rule, the dihydropyrazine units should be positioned as closely to the center of the molecule as possible to form equally large aromatic systems on the two sides.

Miao and co-workers^[13] prepared the isomeric compounds **6** and **7** (Figure 1), and could show that the NH units in **7** are much more shielded than those in **6**, as demonstrated by NMR spectroscopic and UV/Vis studies. Both isomers are persistent.



Uwe Bunz completed his PhD in 1991 (Prof. G. Szeimies; LMU Munich), carried out postdoctoral research at UC Berkeley (1991–1992; Prof. K. P. C. Vollhardt), before completing his Habilitation in Mainz (1997, Prof. K. Müllen). He then became Associate Professor (1997–2001) and then Full Professor (2001–2002) at the University of South Carolina, and then Full Professor at the Georgia Institute of Technology (2003–2010). He is currently Professor (Lehrstuhl I) at the Organisch-Chemische Institut der Ruprecht-Karls-Universität Heidelberg. His research interests include π -conjugated materials.



Benjamin D. Lindner studied chemistry at the Universities of Marburg and Heidelberg (diploma in 2010 with Prof. G. Helmchen on enantioselective synthesis). He is currently carrying out PhD research in the group of U. Bunz, on synthetic approaches towards large *N*-heteroacenes for application in the field of organic electronics.



Jens U. Engelhart studied chemistry in Heidelberg and Bristol (diploma with U. Bunz on the synthesis of novel *N*-Heteroacenes by Pd-catalyzed methods). In August 2011 he started PhD research with U. Bunz, exploring novel synthetic routes towards electron-transporting materials based on *N*-heteroacenes.



Manuel Schaffroth studied chemistry at the Ruprecht-Karls University of Heidelberg and in 2011 completed his MSc with U. Bunz on functionalized fluorubine derivatives. Since December 2011 he has been carrying out PhD research in the same group on the synthesis and properties of large *N*-heteroacenes.

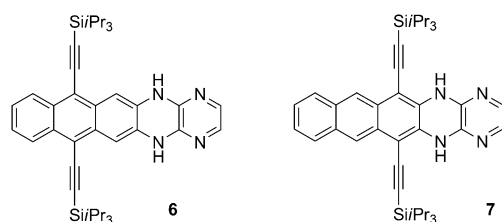


Figure 1. Isomeric dihydrotetraazapentacenes **6** and **7**.

4. Quantum Chemical Calculations

Early on, Chen and Chao^[14] identified a series of aza-substituted pentacenes **8–13** (Figure 2) as potentially suitable materials for n-channel behavior in organic thin-film tran-

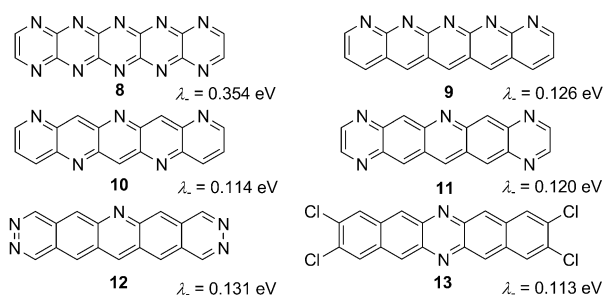


Figure 2. Theoretical study of promising azaacenes by Chao et al.

sistors. These heterocycles all show small reorganization energies λ_- (0.15–0.2 eV) and attractive ionization potentials.

Winkler and Houk^[15] expanded upon this topic and investigated nitrogen-containing acenes in detail; the addition of nitrile substituents, to give **14–19**, would additionally be valuable to drive self-assembly and also lower LUMO energies. The calculated λ_- values ranging between 0.13 and 0.15 eV, similar to those calculated by Chen and Chao for the consanguine targets (Figure 3).

Very recently, Shuai and co-workers^[16] calculated the electronic structure of a series of N-heteroacenes and their *N,N'*-dihydro congeners (Figure 4), with and without TIPS-ethynyl (triisopropylsilylethynyl) groups. The oxidation of the *N,N'*-dihydro compounds leads to a more distinct stabilization

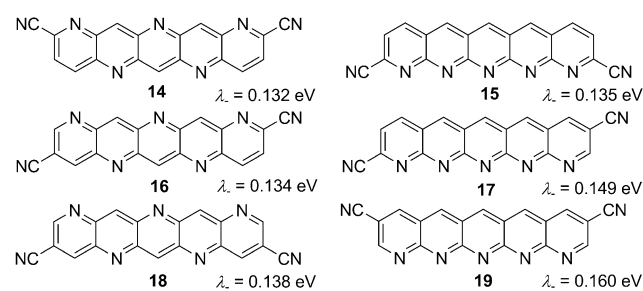


Figure 3. Theoretical study of promising azaacenes by Winkler and Houk.

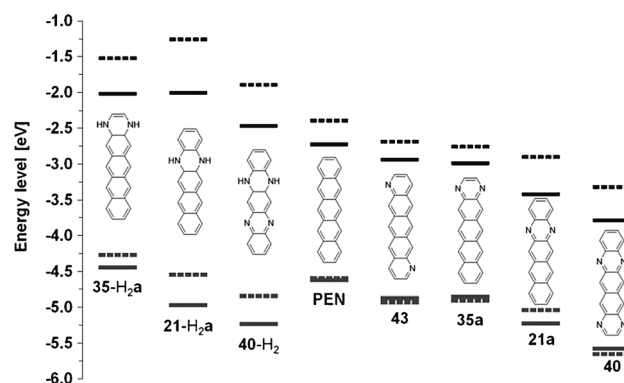


Figure 4. Calculated FMO levels (B3LYP 6-31G*) of selected dihydro-azaacenes according to Shuai and co-workers. —: TIPS-ethynylated compounds, ----: unsubstituted compounds.^[16]

of the LUMO than of the HOMO, thereby resulting in a significantly reduced band gap, and an observed red-shifted absorption band.

The absolute position of the frontier molecular orbitals (FMOs) depends upon the position of the nitrogen atoms in the acene system, which was confirmed for a series of azapentacenes by Miao and co-workers.^[17] They demonstrated that compounds **21a** and **40** with internal pyrazine units feature lower FMO energies than their terminal analogues **35a,b**.

Additionally, Shuai and co-workers found that the reorganization energies are larger in the *N,N'*-dihydro compounds than in the “true” azaacenes. The issue of packing, charge injection, and charge transport has also been investigated theoretically by Chen et al.,^[18] while Kuo and co-workers calculated the ionization potentials and reorganization energies of a series of azaacenes and their relatives.^[19] The λ_- values range between 0.19 and 0.24 eV. Two of the more attractive materials predicted were the octafluoro- and octachlorotetraazapentacenes (**20a,b**; Figure 5). Both were

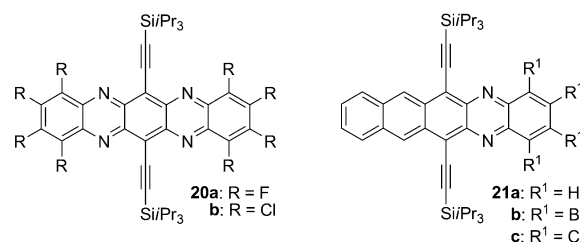


Figure 5. Structures of diversely functionalized azapentacenes **20** and **21**.

calculated to have low reorganization energies and would be easily reduced to the corresponding radical anion.

Of course, one must be aware that charge injection, charge transport, and air stability are not only dependent upon the FMO energy levels of a single azaacene, as the redox properties of single isolated molecules in solution are only loosely related to the many-particle polaron states responsible for charge transport in dense molecular crystals. Also,

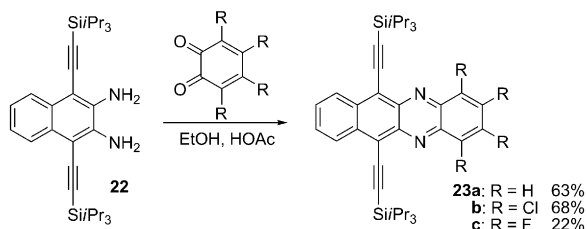
the physical picture of an electron (or positive charge) hopping from molecule to molecule is a very simplified approach, even for ideal crystalline solids without domain boundaries.

Although a significant number of the calculated azaacenes are fascinating targets, there were until recently no good synthetic routes available to prepare them. However, this has changed in the last few years.

5. Syntheses

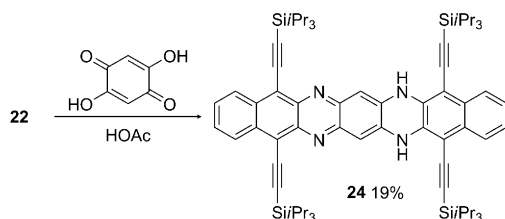
5.1. Direct Condensation Reactions of Diamines with *ortho*-Quinones or Aromatic 1,2-Dihydroxy Compounds

The oldest route to diazaacenes is the condensation of *ortho*-quinones or *ortho*-dihydroxyarenes to *ortho*-diamines to furnish diazapentacenes such as **21** in modest but reliable yields after oxidation of the intermittently formed *N,N'*-dihydro compound.^[20] An attractive synthesis is that of the tetrafluorodiazatetracene **23c**, which forms from **22** and tetrafluorobenzoquinone (Scheme 3).^[21] The yields are mod-



Scheme 3. Diazatetracenes by classical condensation reactions.

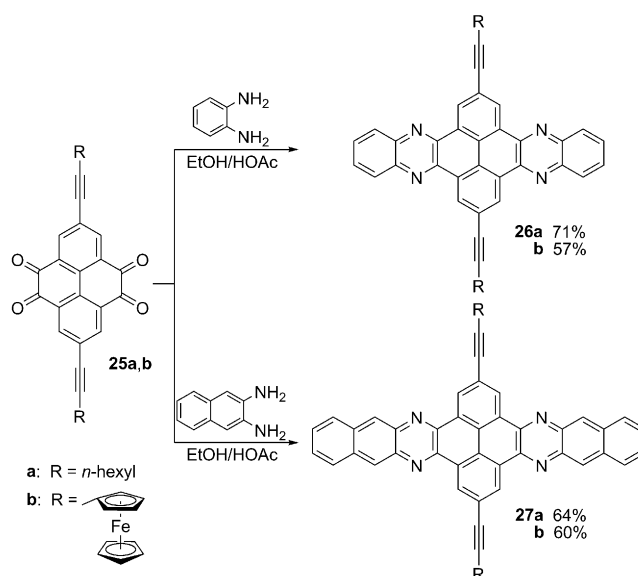
est, as **23c** reacts with ethanol through a nucleophilic aromatic substitution in 25 % yield. The condensation reaction was also used for the construction of **24** by treating **22** with 2,5-dihydroxybenzoquinone (Scheme 4).^[22] Miao and co-workers



Scheme 4. Twofold condensation for the synthesis of **24**.

synthesized **6** (see Figure 1) by condensation of a dihydroxyanthracene derivative with diaminopyrazine.^[13] The direct condensation seems to work if both partners are sterically uncrowded: The TIPS-ethynyl groups in the starting material are relatively far removed from the site of reaction.

The condensation route is generally applicable, but its yields tend to be unsatisfactory. There is an exception though,

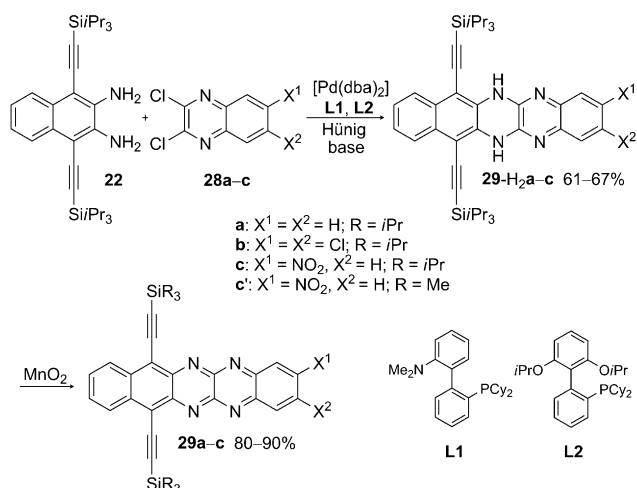


Scheme 5. Synthesis of pyrene-containing azaacenes.

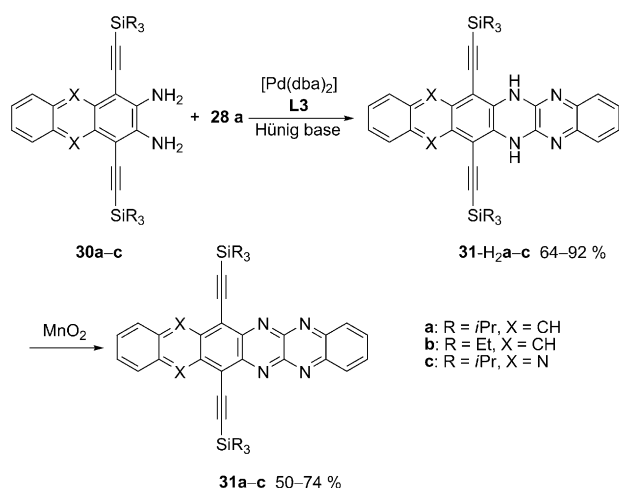
if pyrenetetraone or derivatives such as **25a, b** are employed as the coupling partner (Scheme 5). Mateo-Alonso and co-workers, and earlier Müllen and co-workers, demonstrated the facile construction of large azaacenes with interspersed pyrene units.^[23] The synthesis of **27a, b** and related materials proceeds smoothly, as each diazaacene is separated by the pyrene unit—and in the sense of Clar sextets and aromaticity—isolated from each other. Therefore, there are no issues with the occurrence of NH compounds that always plague the synthesis of the larger linear acenes. The introduction of a pyrene nucleus might also allow the build up of ladder-type polymers containing pyrazine or phenazine units bridged by pyrene units.

5.2. Pd-Catalyzed Coupling Reactions of Aromatic Diamines with Activated Halides: Synthesis of Pentacenes and Hexacenes

A novel approach towards larger azaacenes with up to six nitrogen atoms in the aromatic core deploys a Buchwald coupling.^[24] Coupling of **22** to the activated dichloroquinoxalines **28a–c** under Pd catalysis in Hünig base drives the formation of **29-H₂a–c** in good to excellent yields (Scheme 6). In the same vein, tetraazatetracenes can be obtained.^[25] Attempts to make this reaction occur without Pd catalysis, that is, coupling alone or in the presence of several different bases, were less successful. The oxidation of **29-H₂a–c** with MnO₂ gave rise to the formation of **29a–c**. The construction of the *N,N'*-dihydroazaacenes by Pd catalysis is a powerful method. Substituted quinoxalines couple smoothly to aromatic diamines to give the respective azaacenes after oxidation. It is also possible to prepare tetraza- and hexaazahexacenes with this method.^[26] Instead of using a substituted diaminonaphthalene, one can employ either the disubstituted diaminophenazine **30c** or a disubstituted diaminanthracene such as **30a** or **30b** with the dichloroquinoxaline **28a** (Scheme 7).



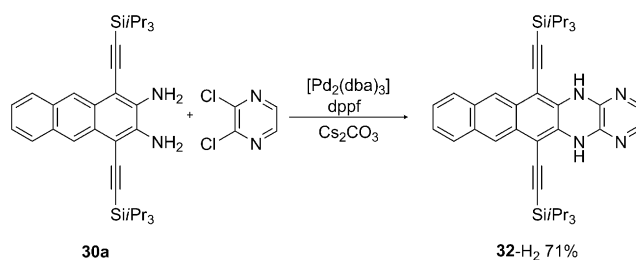
Scheme 6. Pd-catalyzed amination and subsequent oxidation towards **29**.



Scheme 7. Azahexacenes by Pd catalysis.

The Pd-catalyzed coupling furnishes **31a–c** in good to excellent yields after oxidation of **31-H2a–c** with MnO_2 . In the case of the tetraaza- and hexaazahexacenes **31a–c**, TIPS-ethynyl groups suffice to stabilize the hexacene nucleus; silyl groups with larger substituents (*tert*-butyl, trimethylsilyl) are necessary in the case of analogous hydrocarbons to prevent the acenes from dimerizing.^[27]

Pd catalysis was also explored by Miao and co-workers, who prepared the dihydrotetraazatetracene **32-H₂** by coupling diamine **30a** with 2,3-dichloropyrazine in the presence of dppf as a ligand (Scheme 8).^[28] the oxidation of compound **32-H₂** fails in our hands, however,^[21] and we instead observe the formation of a terminal bisamide. Such pyridones are apparently always generated when dihydroazaacenes containing a terminal pyridine ring are treated with MnO_2 .^[29]

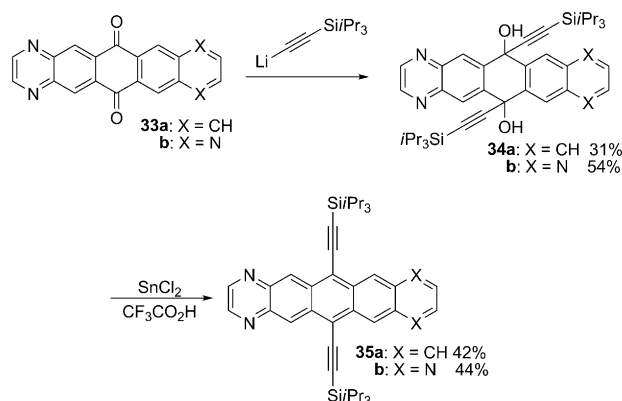


Scheme 8. Pd-mediated formation of **32-H₂**.

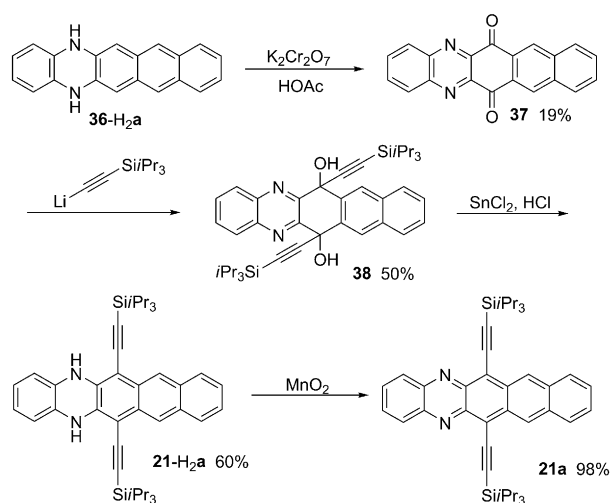
5.3. Other Routes

5.3.1. Quinones

One of the more useful routes is the reaction of quinone precursors^[17,30] such as **33a,b** (Scheme 9), **37**, **39**, **42**, or **45a,b**^[31] with TIPS-ethynyllithium or TIPS-ethynylmagnesium salts, followed by subsequent deoxygenation with tin chloride or $\text{KI}/\text{Na}_2\text{HPO}_2$ in acetic acid to give, for example **40-H₂** (Scheme 11). This method is analogous to that developed by Anthony et al. for the preparation of substituted larger acenes.^[32]

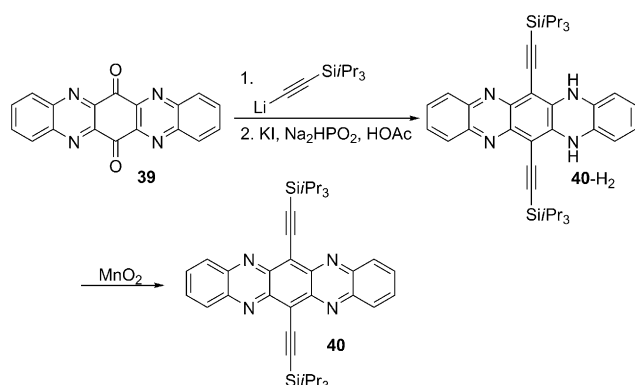


Scheme 9. Ethynylation and deoxygenation of **33** to form **35**.



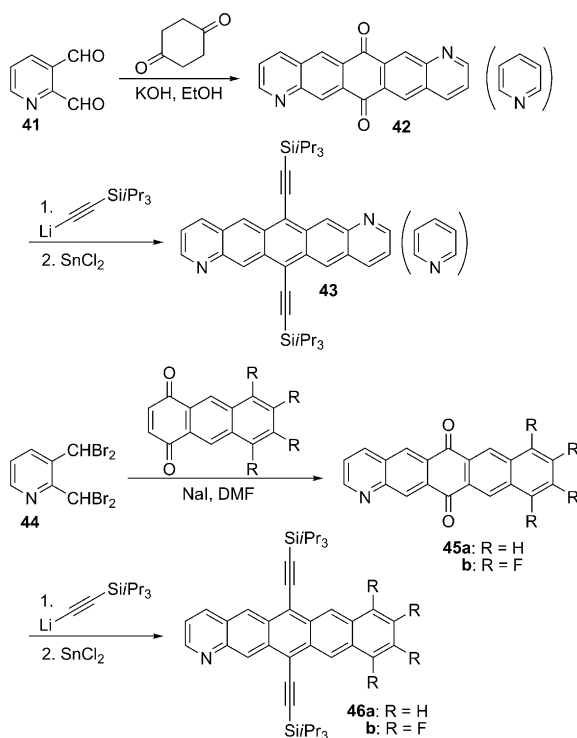
Scheme 10. Formation of **21a** from **36-H₂a**.

In the case of **37** and **39** one isolates **21-H₂a** and **40-H₂**, respectively (Schemes 10 and 11), which are subsequently oxidized by manganese oxide to **21a** and **40**, while the azaacenes form directly in the cases of **33a,b** and **42**. The *N,N'*-dihydro compounds are not observed (Scheme 9).



Scheme 11. Synthesis of the symmetrical tetraazapentacene **40**.

A “conventional” approach to heteroacenes was developed^[33] by Zhang and co-workers who performed a condensation reaction of pyridine-2,3-carboxaldehyde (**41**) with cyclohexanedione or a 1,4-anthraquinone of choice to obtain suitable precursors (Scheme 12), which were alkynylated to give **43** or **46** after deoxygenation with tin dichloride.

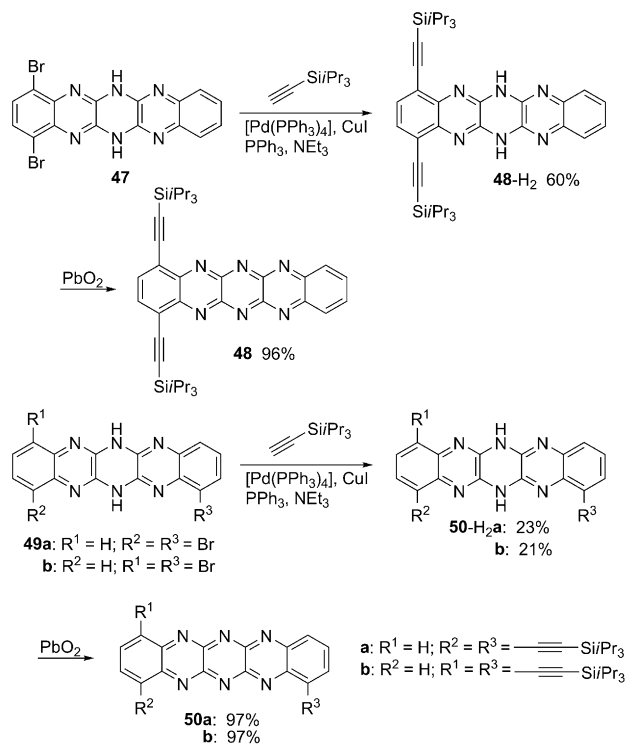


Scheme 12. Synthetic route to molecules **43** and **46a,b**.

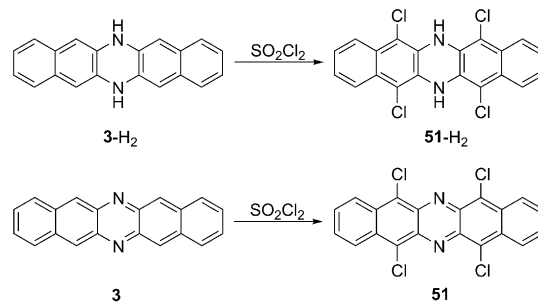
5.3.2. Other Targets, Other Methods

Starting from the dibromides **47** and **49a,b**, Sonogashira reaction gives access to the NH compounds **48-H₂** and **50-H₂a,b**, respectively (Scheme 13). These are electron poor, and can only be oxidized by lead(IV) oxide into the hexaazaacenes **48** and **50a,b**, respectively, which are strong oxidizing agents themselves. This is a remarkable synthesis, as this is a novel motif for azaacenes in which three consecutive rings carry pyrazine units—an attractive concept, even if **48** is not particularly stable.^[34]

Fleischhauer et al. prepared a series of *N,N'*-dihydrohexaazapentacenes and investigated the properties of the *N*-arylated compounds.^[35] Oxidation is not possible in such cases. An important approach is the functionalization of heteroacenes. Both **3-H₂** and also **3** are chlorinated by SO₂Cl₂ to give the tetrachlorinated species **51-H₂** and **51**, respectively, without degradation of the nucleus (Scheme 14).^[36] This is one of the few reactions that are reported for heteroacenes.



Scheme 13. Synthesis of nitrogen-rich azapentacenes **48** and **50**.

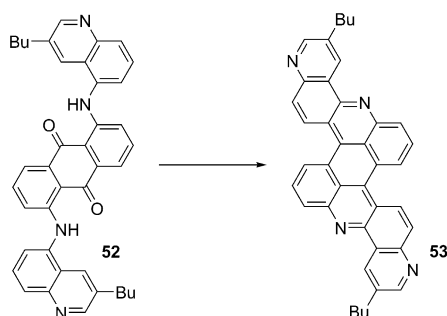


Scheme 14. Chlorination of **3-H₂** and **3** by sulfuryl chloride.

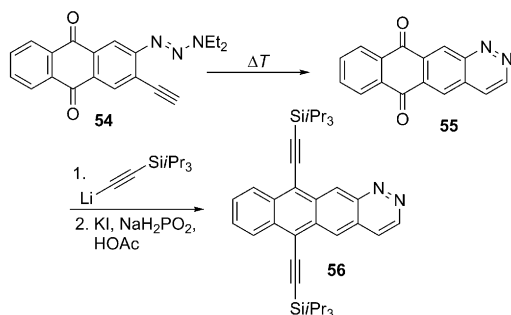
Azaacenes do not have to be linear.^[37] Sarkar, Bock et al. (Scheme 15) obtained tetraazaacene **53** by electrophilic cyclization of the precursor **52**. Acene **53** should have great potential as an active material in organic electronic devices such as thin-film transistors.

An attractive approach towards unknown naphtho-substituted cinnolines was reported by Haley and co-workers (Scheme 16).^[38] Pyrolysis of the precursor **54** furnished **55**, which upon alkylation and deoxygenation under Miao-Bunz conditions gave the desired compound **56**. This is the first example in which an enlarged substituted cinnoline has been produced.

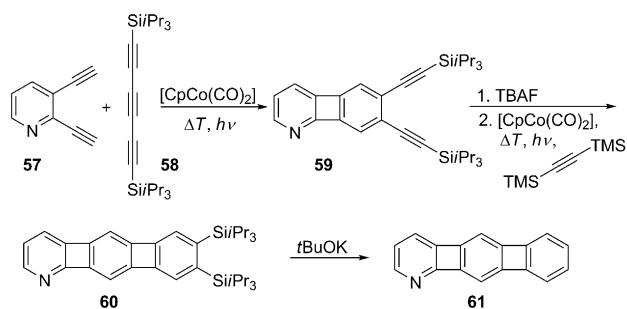
Vollhardt and co-workers^[39] investigated the introduction of four-membered rings into linear azaacenes. Cobalt-catalyzed [2+2+2] cycloaddition of **57** with the triyne **58** afforded the biphenylene precursor **59**, which upon deprotection and



Scheme 15. Extended bent N-heteroacene by acid-promoted dihydrocyclization.



Scheme 16. Cinnoline-containing heteroacenes synthesized by Haley et al.

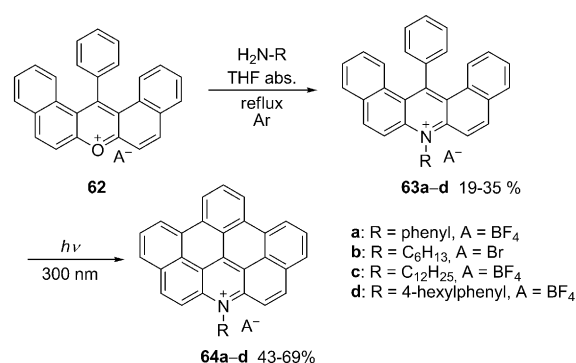


Scheme 17. Synthesis of **61** by twofold cyclotrimerization.

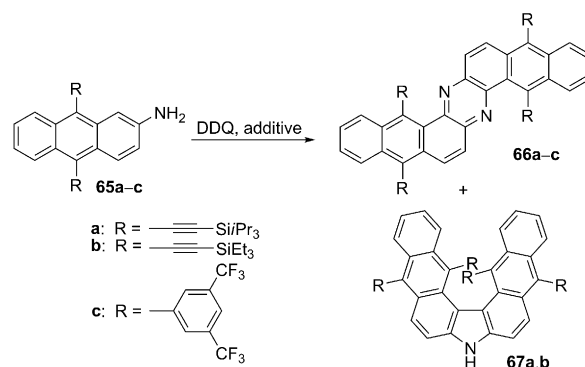
a second cobalt-mediated [2+2+2] cycloaddition transforms into **61** after desilylation (Scheme 17). A crystal structure shows that **61** packs in a fascinating gridlike structure and that compound **61** absorbs at $\lambda_{\text{max}} = 433$ nm in solution.

Other forms of azaacenes were prepared by Müllen and co-workers.^[40] Reaction of the xanthenylium salt **62** with a primary amine in dry THF produces the acridinium salts **63a–d**, which upon irradiation transform into **64a–d** in good to excellent yields (Scheme 18). Some of these salts form nano-objects such as fibers, as well as helical aggregates.

A creative way to obtain “kinked” azaacenes is the oxidation of aminoanthracenes such as **65a–c**, which leads to substituted dinaphtho[2,3-*a*:2',3'-*h*]phenazines **66a–c** in respectable yields. The also attractive azahelicene derivatives **67a,b** were isolated as side products (Scheme 19).^[41] Crystal structure analyses demonstrated that **66a–c** were planar, as expected, while **67a,b** were significantly twisted.

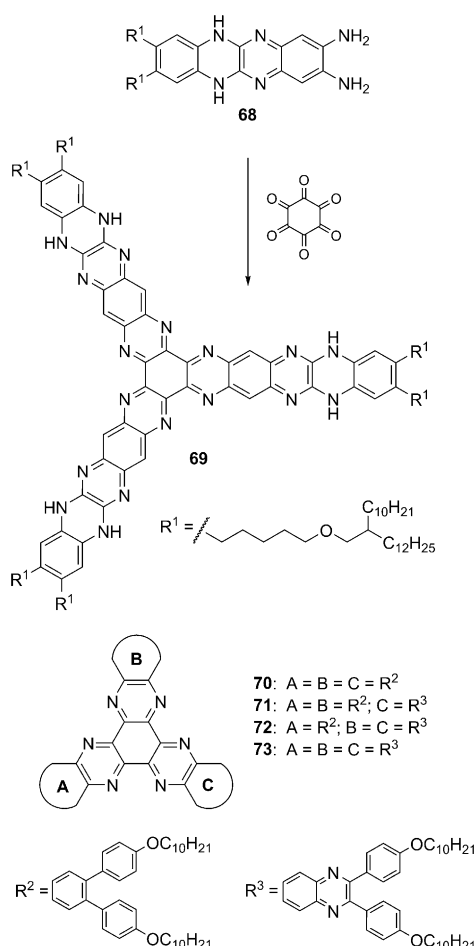


Scheme 18. Annulated acridinium salts by photoactivation.



Scheme 19. Oxidative dimerization of aminoarenes **65** to the kinked heteroacene **66** and the twisted carbazole derivative **67**.

Wudl, Zhang, and co-workers developed an attractive cycloaddition-based route towards novel heteroacenes containing cyclic amides.^[42] Materials with similar structures, however, can also be obtained by direct oxidation of suitable heteroacenes by using MnO_2 ; terminal pyridine groups in large azaacenes are quite susceptible towards oxidation into six-membered lactams.^[29]



Scheme 20. Star-shaped heteroacenes by condensation.

Azaacenes are motifs in hexaazatriphenylenes (HAT-NAs) such as **69–73**.^[43,44] These were obtained by condensation of a suitable diamine such as **68** with either rhodizonic acid or the octahydrate of hexaoxocyclohexane.^[45] If performed correctly, one can also add the amines in a stepwise fashion, so that unsymmetrical targets such as **71** and **72** can be obtained. Solubilizing side chains make the “tristar” molecules processable (Scheme 20).

6. Optical, Electronic, and Electrochemical Properties of N-Heteroacenes

6.1. Reduced Versus Oxidized Heteroacenes

Generally, *N,N'*-dihydro compounds such as **3-H₂** and **5-H₂** display a much higher band gap (reflected in the UV/Vis and emission spectra) than the corresponding fully oxidized heteroacenes **3** and **5**. Calculations and single-crystal X-ray structures show the planar dihydropyrazine units interrupt the electronic coupling between the aromatic units they interconnect. As a consequence, both the absorption and emission are blue-shifted. This is interesting, as the HOMO of **3-H₂** (Figure 6) is fully extended over the whole molecule, while the LUMO appears to be constructed of two independ-

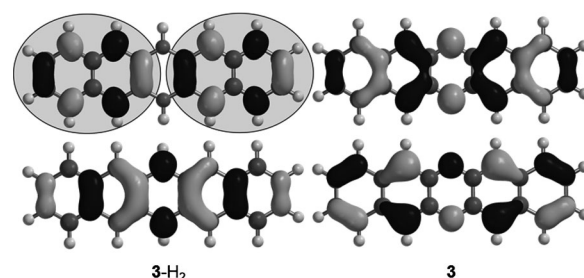


Figure 6. Calculated HOMO (bottom) and LUMO (top; B3LYP 6-311 + G**) of NH compound **3-H₂** (left) and the heteroacene **3** (right).

ent naphthalene units (emphasized by gray ellipses in Figure 6). Upon oxidation, the HOMO of **3** is less stabilized than the LUMO when compared to the FMOs of **3-H₂**, thus leading to a much smaller gap. This is in agreement with the theoretical studies outlined in Figure 4.^[16] So both the Clar rule and also MO theory predict blue-shifted absorption and emission for the NH compounds compared to those of the oxidized species.

6.2. Linear Heteroacenes

Linear azapentacenes are derivatives of pentacene in which one or more CH groups are substituted by nitrogen atoms to form pyridine or pyrazine rings. The absorption and emission spectra of the symmetrical tetraazapentacene **40** are very similar to those recorded for the analogous bis[(triisopropylsilyl)ethynyl]pentacene (TIPSPEN). If TIPSPEN is substituted by halogens, only a small bathochromic shift in the absorption and emission bands is observed, as is expected, as halogen substituents barely and rarely change the optical properties of arenes and acenes.

Transposition of two of the four nitrogen atoms with the C–C≡C–TIPS-ethynyl units in the nucleus of **40** leads to heteroacene **29a**. The absorption band of this heteroacene is red-shifted by 67 nm (Figure 7) and is barely fluorescent. This effect is much stronger if acceptor substituents are attached to the right-hand part of the tetraazapentacene, as in **29b,c** (see Scheme 6). A similar effect is also observable for diazaacenes, which also show a red-shift of their absorption upon electro-negative substitution of the core.

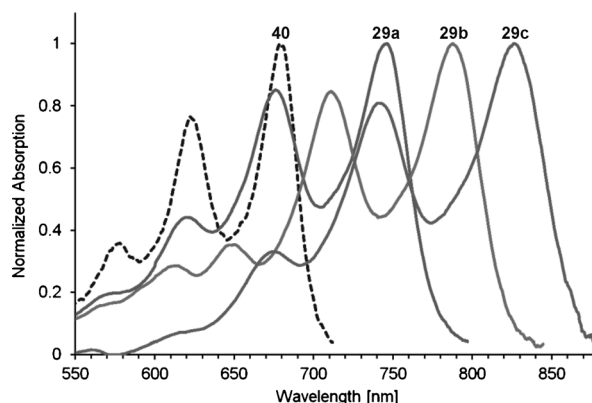


Figure 7. Absorption spectra of tetraazapentacenes **29a–c** and **40**.

Quantum chemical calculations support this trend and explain why this red-shift is observed. For **40**, the HOMO and the LUMO are regularly distributed over the entire aromatic core, that is, congruent.^[46] That is no longer the case in the acceptor-substituted heteroacenes **29a–c**. The HOMO and LUMO plots for the nitro compound **29c** (Figure 8) reveal

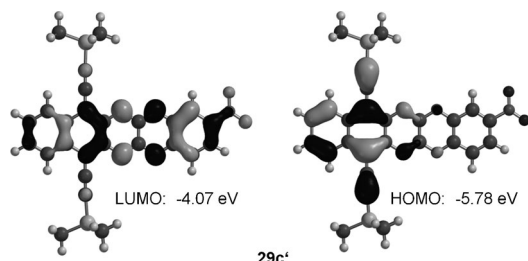


Figure 8. Calculated FMOs of **29c'**. The $\text{Si}i\text{Pr}_3$ groups are substituted by TMS groups.

that the LUMO is equally distributed over the whole molecule, but the HOMO is located on the left-hand side, which does not carry the electronegative substituent. Consequently, the nitro group is less efficient in stabilizing the HOMO than lowering the energy of the LUMO. As a consequence, the HOMO–LUMO gap decreases, which is entirely consistent with the observed red-shift in the absorptions spectrum. The observed extinction coefficients for λ_{max} also decrease, as the HOMO–LUMO overlap (as calculated) decreases with electronegative substitution.

Organic electron-transport materials have been less intensively researched than their hole-transporting analogues.^[47] The n-semiconductors would be useful for both active elements in thin-film transistors and also as possible C_{60} substitutes in OPV devices. A necessary, but not sufficient, condition for success is a LUMO level that is positioned as low or lower than that of C_{60} . Cyclic voltammetric studies (Figure 9) show that most of the heteroacenes show this behavior.

When we first started our research into heteroacenes, we found that they were all easily and reversibly reduced in cyclic voltammetric experiments into their monoanions or even dianions. The experimental reduction potentials (Figure 9) correlate very well with the calculated LUMO energies (B3LYP 6-311+G**), with the slope of the graph being -0.87 ; there is an almost 1:1 empirical correlation between the calculated LUMO position and first reduction potential. The best-fit line allows the first reduction potential of specific heteroacenes to be predicted by quantum chemical calculations. The symmetrical tetraazaacene **40**, for example, shows a first reduction potential at -0.79 eV versus ferrocene and a calculated LUMO position of -3.8 eV, which suggests that it should be suitable for organic electronics applications. Furthermore, its radical anion should not be able to reduce oxygen, that is, it should be stable in air. Most azaacenes (>4 rings, >2 nitrogen atoms or 2 nitrogen atoms + electronegative substituents) fulfill this condition and are, therefore, potential candidates as electron-transporting materials.

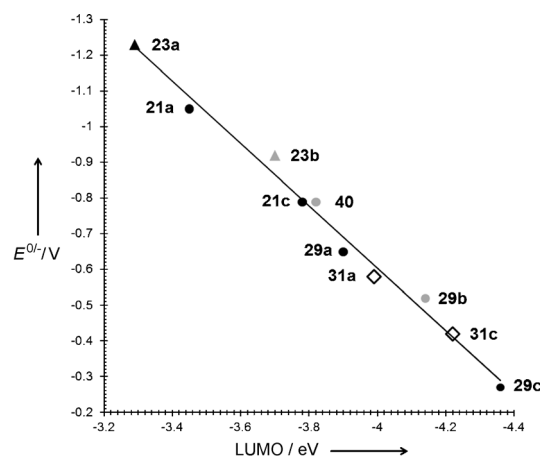


Figure 9. Empirical correlation between theoretical LUMO energies and experimental first reduction potentials of various azaacenes.

7. Structures and Supramolecular Ordering

An important aspect of the larger heteroacenes is their supramolecular solid-state ordering. Ariga, Hill, and co-workers have reviewed the self-assembly and solid-state structures of some long-chain alkoxy-substituted larger heteroacenes.^[4d] Very recently Lee and co-workers investigated the self-assembly of **74a–c**; These form gels with attractive structures from different organic solvents, as shown for **74c** in Figure 10.^[48]

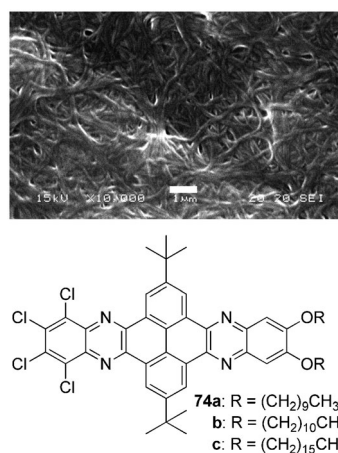


Figure 10. Self-assembly (left) and structure (right) of **74**. SEM micrograph reproduced with permission from the American Chemical society.^[48] Scale bar = $1\ \mu\text{m}$.

Crystallization rather than gelation is observed with related compounds. For example, the crystallization of **75e,f**^[49] leads to stranded morphologies (Figure 11).

The formation of these supramolecular structures is a privilege of these planar cores substituted with several long alkoxy chains; in most cases the long chains are attached laterally, that is, to the terminal rings of the molecular scaffold (Figure 11), which seems to enforce the acenes to pack on top of each other. If more compact substituents such as TIPS-

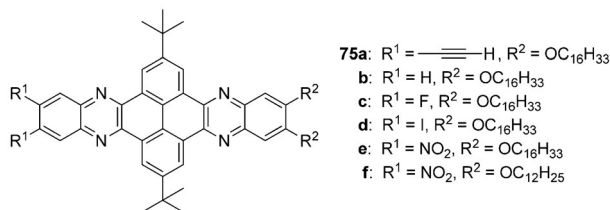
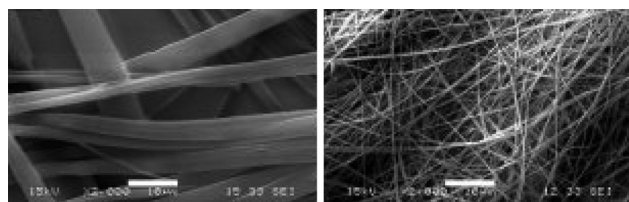


Figure 11. SEM images of the self-assembly of **75e** (top left) and **75f** (top right). Structures of **75a–f** (bottom).^[49] Reprinted with permission from Wiley-VCH. Scale bars = 10 μm .

ethynyl are introduced at the center of the heteroacene core, one invariably ends up with well-developed single-crystalline specimens that, with few exceptions, display a packing that is similar to that of TIPSPEN, particularly when the $4n + 2\pi$ azaacenes are considered.^[32,50]

These brickwall motives are also observed for N,N' -dihydrooligoazaacenes, but are not nearly as prevalent. In several cases, one finds dimeric structures, herringbone types, or more complex solid-state packing.^[51] However, compound **3-H₂** shows a herringbone motif similar to that observed for pentacene. The $4n + 2\pi$ systems are more interesting than the N,N' -dihydroazaacenes for organic electronics, as they are potentially capable of electron transport and most of these display the desired 2D packing found in TIPSPEN.

8. Applications of N-Heteroacenes in Organic Electronics: Ideal Materials for Electron Transport?

N-heteroacenes have been of interest for organic electronics since Nuckolls and co-workers demonstrated that **36-H₂a** (Figure 12) was a viable substitute for pentacene as active hole transporting layers. In thin-film transistors, μ_+ values up to $6 \times 10^{-3} \text{ cm}^2 \text{ V}^{-1} \text{ s}^{-1}$ were measured.^[10] Other derivatives of the NH compounds, for example tetrachloride **51-H₂**, displayed hole-transporting properties

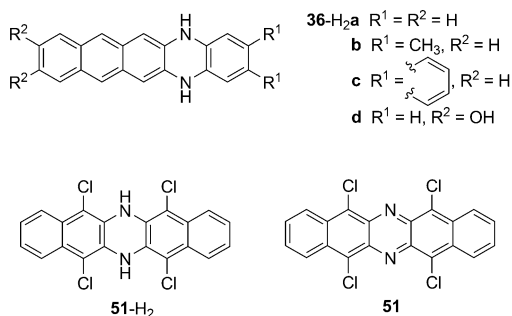


Figure 12. Structures of processed materials **36-H₂**, **52**, and **52-H₂**.

($1.4 \text{ cm}^2 \text{ V}^{-1} \text{ s}^{-1}$), while its oxidized derivative **51** surprisingly was an acceptable hole-transporting material ($0.1\text{--}0.13 \text{ cm}^2 \text{ V}^{-1} \text{ s}^{-1}$).^[36]

Zhang and co-workers^[33] described the first use of (oxidized) N-heteroacenes, such as **43** and **46a–c** (Figure 13), as viable electron-transport materials with mobilities of

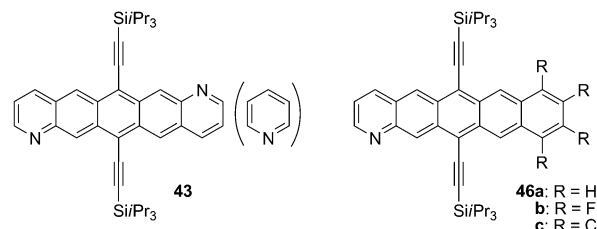


Figure 13. Structures of **43** and **46**.

$0.11 \text{ cm}^2 \text{ V}^{-1} \text{ s}^{-1}$ (μ_+ hole) and $0.15 \text{ cm}^2 \text{ V}^{-1} \text{ s}^{-1}$ (μ_- electrons) for **43**, and $0.08 \text{ cm}^2 \text{ V}^{-1} \text{ s}^{-1}$ (μ_+ hole)/ $0.09 \text{ cm}^2 \text{ V}^{-1} \text{ s}^{-1}$ (μ_- electrons) for the tetrafluoride **46b**. Substitution of Cl for F in **46c** resulted in the ambipolar mobilities increasing to $0.12 \text{ cm}^2 \text{ V}^{-1} \text{ s}^{-1}$ (μ_+)/ $0.14 \text{ cm}^2 \text{ V}^{-1} \text{ s}^{-1}$ (μ_-).

How do these transistors work and what is their secret? All of the heteroacenes are vapor deposited, typically on octadecyltrimethoxysilane (OTS) treated silicon oxide on silicon as a gate. The evaporation of the heteroacene semiconductor on a smooth pretreated surface leads to evaporated films of good quality that will later efficiently transport charges. The temperature of the substrate plays a significant role in the formation of the crystal film and has to be controlled. To finish the transistor, a mask is placed on the semiconductor layer and the metal (gold, silver, etc.) source and drain electrodes are evaporated on top of the films in the desired configurations (Figure 14). This bottom-gate-top-

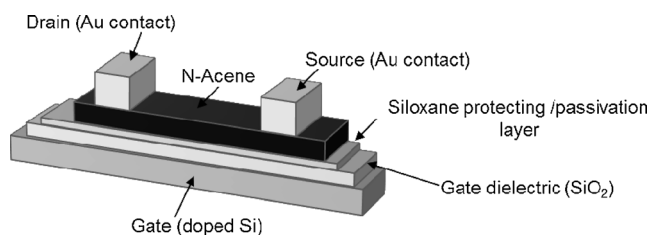


Figure 14. Assembly of a bottom-gate-top-contact thin-film transistor.

contact geometry is the most often employed configuration to obtain good mobilities, even for single crystals that are grown from solution.

The most useful azaacene to date is **40** prepared by us in 2009^[31] and exploited by Miao et al.^[30,52] as the active layer in thin-film transistors. Evaporation of **40** on a platform as shown in Figure 15 followed by evaporation of the gold top-contacts produces working thin-film transistors that display electron transport. Electron mobilities of up to $3.3 \text{ cm}^2 \text{ V}^{-1} \text{ s}^{-1}$ ($0.5 \text{ cm}^2 \text{ V}^{-1} \text{ s}^{-1}$ in air) were measured. Processing **40** from chlorobenzene onto an OTS-functionalized surface fails

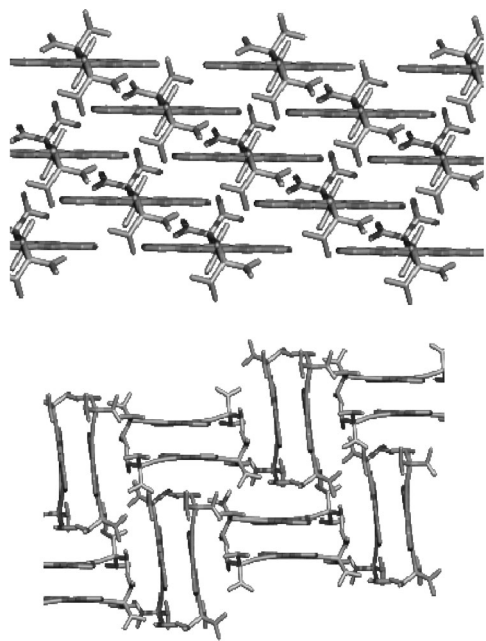


Figure 15. Examples of crystal morphologies: Brickwall motif of **40** (left) and sandwich herringbones of **35b** (right).

because of the lack of wetting of the pretreated SiO₂ dielectric. When the semiconductor **40** is directly solution processed onto silicon dioxide instead, the wetting is better, but the mobility drops to 0.003 cm² V⁻¹ s⁻¹. This is attributable to the trapping of the negative charge by the Si–OH groups.

To solve the problem of solution processing, single crystals of **40** were grown on OTS-treated Si/SiO₂ and silver strips were glued onto the formed specimen. Mobilities of up to 1.8 cm² V⁻¹ s⁻¹ were measured in a thin-film transistor configuration. This interesting result is, however, unfavorable for application as, in contrast to solution or vapor deposition, automated fabrication of devices is very difficult.

When **35b**—an isomer of **40**, where the four nitrogen atoms sit at the terminal rings—is evaporated to give thin-film transistors under otherwise identical conditions, the electron mobility μ_{-} drops to 0.3–1.1 cm² V⁻¹ s⁻¹.^[17] There are probably two reasons for the decreased performance: 1) The LUMO of **35b** is around 0.3 eV higher in energy than that of **40**. 2) The molecular packing of **35b** is not in the preferred 2d brickwall motif, as is adopted by **40** (and also by TIPSPEN), but a sandwich herringbone, in which the interaction of the molecules is apparently reduced.

The dramatic change in the packing when going from **40** to **35b** was unexpected, but can be rationalized by the exposed N atoms of the terminal rings in **35b** undergoing hydrogen bonding, which then leads to the observed, but surprising packing (Figure 15)—a sandwich herringbone structure. An additional consequence of the molecular structure is that **35b** functions as an ambipolar thin-film transistor with a hole mobility μ_{+} of 0.05–0.22 cm² V⁻¹ s⁻¹.

Overall, **40** is currently by far the best of all the tested heteroacenes with respect to electron-transport properties in thin-film transistors. With top contacts, both vapor-deposited

as well as single-crystalline (solution grown) preparations of **40** are attractive with spectacular electron mobilities.

Azapentacenes with the same number of nitrogen atoms display comparable properties. Consequently they allow a deep understanding to be gained of how differences in intermolecular orientation (induced by slight changes in the molecules) determine mobilities.

9. Conclusions and Outlook

Azaacenes, be it in their *N,N'*-dihydro form or as fully oxidized $4n + 2\pi$ systems, have been known for a long time, with NH compounds dating back to the end of the 19th century. However, only recently have significant efforts been devoted to prepare substituted and, therefore, processable and characterizable derivatives. Consequently, the dramatic differences in the electronic properties of the reduced and oxidized species could be explained. In the last three years, new and powerful synthetic approaches to the larger heteroacenes have been developed. In particular, the Pd-catalyzed coupling of diamines to activated aromatic dihalides now makes a significant number of novel azaacenes easily available. At the same time new, bent and tripodal heteroacenes were described. The chemical behavior, self-assembly, spectroscopy, electrochemical, and electric properties of azaacenes are clearly different from those of their acene congeners. Increased oxidative stability, the presence of an oxidized and a reduced form, as well as the potential for tautomers further increases the gamut of molecules with different properties that can be achieved.

The most spectacular development to date is the use of the symmetrical tetraazapentacene **40** as an electron-transport material in organic thin-film transistors, which demonstrates electron mobilities μ_{-} of up to 3.3 cm² V⁻¹ s⁻¹ from vapor-deposited layers. Overall, the field of N-heteroacenes is awaking from its hibernation. Opportunities lie in the synthesis of larger azaacenes, such as the synthesis of stable $4n + 2\pi$ oligoazaheptacenes and -octacenes, the attachment of different substituents, and also the development of novel synthetic methods to achieve all of this.

We thank the Deutschen Forschungsgemeinschaft for generous financial support (DFG-Bu771-1) and the Deutschen Telekom Stiftung.

Received: November 27, 2012

Published online: February 18, 2013

- [1] O. D. Jurchescu, J. Baas, T. T. M. Palstra, *Appl. Phys. Lett.* **2004**, *84*, 3061–3063.
- [2] a) J. E. Anthony, *Angew. Chem.* **2008**, *120*, 460–492; *Angew. Chem. Int. Ed.* **2008**, *47*, 452–483; b) J. E. Anthony, *Chem. Rev.* **2006**, *106*, 5028–5048.
- [3] a) Y. Sakamoto, T. Suzuki, M. Kobayashi, Y. Gao, Y. Fukai, Y. Inoue, F. Sato, S. Tokito, *J. Am. Chem. Soc.* **2004**, *126*, 8138–8140; b) C. R. Swartz, S. R. Parkin, J. E. Bullock, J. E. Anthony, A. C. Mayer, G. G. Malliaras, *Org. Lett.* **2005**, *7*, 3163–3166;

- c) M. L. Tang, J. H. Oh, A. D. Reichardt, Z. Bao, *J. Am. Chem. Soc.* **2009**, *131*, 3733–3740.
- [4] a) U. H. F. Bunz, *Pure Appl. Chem.* **2010**, *82*, 953–968; b) U. H. F. Bunz, *Chem. Eur. J.* **2009**, *15*, 6780–6789; c) Q. Miao, *Synlett* **2012**, 326–336; d) G. J. Richards, J. P. Hill, T. Mori, K. Ariga, *Org. Biomol. Chem.* **2011**, *9*, 5005–5017.
- [5] a) E. Clar, F. John, *Chem. Ber.* **1929**, *62*, 3021–3029; b) E. Clar, F. John, *Chem. Ber.* **1930**, *63*, 2967–2977; c) E. Clar, F. John, *Chem. Ber.* **1931**, *64*, 981–988.
- [6] O. Hinsberg, *Justus Liebigs Ann. Chem.* **1901**, *319*, 257–286.
- [7] a) O. Fischer, E. Hepp, *Chem. Ber.* **1890**, *23*, 2789–2793; b) O. Fischer, E. Hepp, *Chem. Ber.* **1895**, *28*, 293–301.
- [8] F. Kummer, H. Zimmermann, *Ber. Bunsen-Ges.* **1967**, *71*, 1119–1125.
- [9] E. Leete, O. Ekechukwu, P. Delvigs, *J. Org. Chem.* **1966**, *31*, 3734–3739.
- [10] Q. Miao, T. Q. Nguyen, T. Someya, G. B. Blanchet, C. Nuckolls, *J. Am. Chem. Soc.* **2003**, *125*, 10284–10287.
- [11] J. I. Wu, C. S. Wannere, Y. Mo, P. von R. Schleyer, U. H. F. Bunz, *J. Org. Chem.* **2009**, *74*, 4343–4349.
- [12] Q. Tang, J. Liu, H. S. Chan, Q. Miao, *Chem. Eur. J.* **2009**, *15*, 3965–3969.
- [13] Z. He, D. Liu, R. Mao, Q. Tang, Q. Miao, *Org. Lett.* **2012**, *14*, 1050–1053.
- [14] H.-Y. Chen, I. Chao, *ChemPhysChem* **2006**, *7*, 2003–2007.
- [15] M. Winkler, K. N. Houk, *J. Am. Chem. Soc.* **2007**, *129*, 1805–1815.
- [16] X.-D. Tang, Y. Liao, H. Geng, Z.-G. Shuai, *J. Mater. Chem.* **2012**, *22*, 18181–18191.
- [17] Z. Liang, Q. Tang, R. Mao, D. Liu, J. Xu, Q. Miao, *Adv. Mater.* **2011**, *23*, 5514–5518.
- [18] X.-K. Chen, J.-F. Guo, L.-Y. Zou, A.-M. Ren, J.-X. Fan, *J. Phys. Chem. C* **2011**, *115*, 21416–21428.
- [19] C.-H. Li, C.-H. Huang, M.-Y. Kuo, *Phys. Chem. Chem. Phys.* **2011**, *13*, 11148–11155.
- [20] A. L. Appleton, S. M. Brombosz, S. Barlow, J. S. Sears, J. L. Bredas, S. R. Marder, U. H. F. Bunz, *Nat. Commun.* **2010**, *1*, 91.
- [21] B. D. Lindner, J. U. Engelhart, M. Märken, O. Tverskoy, A. L. Appleton, F. Rominger, K. I. Hardcastle, M. Enders, U. H. F. Bunz, *Chem. Eur. J.* **2012**, *18*, 4627–4633.
- [22] A. L. Appleton, S. Barlow, S. R. Marder, K. I. Hardcastle, U. H. F. Bunz, *Synlett* **2011**, 1983–1986.
- [23] a) S. More, R. Bhosale, S. Choudhary, A. Mateo-Alonso, *Org. Lett.* **2012**, *14*, 4170–4173; b) K. K. McGrath, K. Jang, K. A. Robins, D.-C. Lee, *Chem. Eur. J.* **2009**, *15*, 4070–4077; c) A. Mateo-Alonso, N. Kulisic, G. Valenti, M. Marcaccio, F. Paolucci, M. Prato, *Chem. Asian J.* **2010**, *5*, 482–485; d) B. X. Gao, M. Wang, Y. X. Cheng, L. X. Wang, X. B. Jing, F. S. Wang, *J. Am. Chem. Soc.* **2008**, *130*, 8297–8306; e) Y. Fogel, M. Kastler, Z. H. Wang, D. Andrienko, G. J. Bodwell, K. Müllen, *J. Am. Chem. Soc.* **2007**, *129*, 11743–11749.
- [24] D. S. Surry, S. L. Buchwald, *Chem. Sci.* **2011**, *2*, 27–50.
- [25] O. Tverskoy, F. Rominger, A. Peters, H.-J. Himmel, U. H. F. Bunz, *Angew. Chem.* **2011**, *123*, 3619–3622; *Angew. Chem. Int. Ed.* **2011**, *50*, 3557–3560.
- [26] B. D. Lindner, J. U. Engelhart, O. Tverskoy, A. L. Appleton, F. Rominger, A. Peters, H.-J. Himmel, U. H. F. Bunz, *Angew. Chem.* **2011**, *123*, 8747–8750; *Angew. Chem. Int. Ed.* **2011**, *50*, 8588–8591.
- [27] M. M. Payne, S. R. Parkin, J. E. Anthony, *J. Am. Chem. Soc.* **2005**, *127*, 8028–8029.
- [28] See Ref. [13].
- [29] J. U. Engelhart, B. D. Lindner, O. Tverskoy, F. Rominger, U. H. F. Bunz, *Org. Lett.* **2012**, *14*, 1008–1011.
- [30] Z. Liang, Q. Tang, J. Xu, Q. Miao, *Adv. Mater.* **2011**, *23*, 1535–1539.
- [31] S. Miao, A. L. Appleton, N. Berger, S. Barlow, S. R. Marder, K. I. Hardcastle, U. H. F. Bunz, *Chem. Eur. J.* **2009**, *15*, 4990–4993.
- [32] J. E. Anthony, J. S. Brooks, D. L. Eaton, S. R. Parkin, *J. Am. Chem. Soc.* **2001**, *123*, 9482–9483.
- [33] a) Y.-Y. Liu, C.-L. Song, W.-J. Zeng, K.-G. Zhou, Z.-F. Shi, C.-B. Ma, F. Yang, H.-L. Zhang, X. Gong, *J. Am. Chem. Soc.* **2010**, *132*, 16349–16351; b) C.-L. Song, C.-B. Ma, F. Yang, W.-J. Zeng, H.-L. Zhang, X. Gong, *Org. Lett.* **2011**, *13*, 2880–2883.
- [34] Z. He, R. Mao, D. Liu, Q. Miao, *Org. Lett.* **2012**, *14*, 4190–4193.
- [35] J. Fleischhauer, S. Zahn, R. Beckert, U.-W. Grummt, E. Birkner, H. Görls, *Chem. Eur. J.* **2012**, *18*, 4549–4557.
- [36] S.-Z. Weng, P. Shukla, M.-Y. Kuo, Y.-C. Chang, H.-S. Sheu, I. Chao, Y.-T. Tao, *ACS Appl. Mater. Interfaces* **2009**, *1*, 2071–2079.
- [37] P. Sarkar, I.-R. Jeon, F. Durola, H. Bock, *New J. Chem.* **2012**, *36*, 570–574.
- [38] B. S. Young, J. L. Marshall, E. MacDonald, C. L. Vonnegut, M. M. Haley, *Chem. Commun.* **2012**, *48*, 5166–5168.
- [39] V. Engelhardt, J. G. Garcia, A. A. Hubaud, K. A. Lyssenko, S. Spyroudis, T. V. Timofeeva, P. Tongwa, K. P. C. Vollhardt, *Synlett* **2011**, 280–284.
- [40] D. Wu, W. Pisula, M. C. Haberecht, X. Feng, K. Müllen, *Org. Lett.* **2009**, *11*, 5686–5689.
- [41] K. Goto, R. Yamaguchi, S. Hiroto, H. Ueno, T. Kawai, H. Shinokubo, *Angew. Chem.* **2012**, *51*, 10333–10336; *Angew. Chem. Int. Ed.* **2012**, *124*, 10479–10482.
- [42] G. Li, H. M. Duong, Z. Zhang, J. Xiao, L. Liu, Y. Zhao, H. Zhang, F. Huo, S. Li, J. Ma, F. Wudl, Q. Zhang, *Chem. Commun.* **2012**, *48*, 5974–5976.
- [43] B. R. Kaafarani, T. Kondo, J. S. Yu, Q. Zhang, D. Dattilo, C. Risko, S. C. Jones, S. Barlow, B. Domercq, F. Amy, A. Kahn, J. L. Bredas, B. Kippelen, S. R. Marder, *J. Am. Chem. Soc.* **2005**, *127*, 16358–16359.
- [44] C. Tong, W. Zhao, J. Luo, H. Mao, W. Chen, H. S. O. Chan, C. Chi, *Org. Lett.* **2012**, *14*, 494–497.
- [45] M. Wang, Y. Li, H. Tong, Y. Cheng, L. Wang, X. Jing, F. Wang, *Org. Lett.* **2011**, *13*, 4378–4381.
- [46] A. J. Zuccherro, P. L. McGrier, U. H. F. Bunz, *Acc. Chem. Res.* **2010**, *43*, 397–408.
- [47] a) S. C. Martens, U. Zschieschang, H. Wadepohl, H. Klauk, L. H. Gade, *Chem. Eur. J.* **2012**, *18*, 3498–3509; b) C. Wang, H. Dong, W. Hu, Y. Liu, D. Zhu, *Chem. Rev.* **2012**, *112*, 2208–2267.
- [48] K. Jang, L. V. Brownell, P. M. Forster, D.-C. Lee, *Langmuir* **2011**, *27*, 14615–14620.
- [49] See Ref. [23b].
- [50] J. E. Anthony, D. L. Eaton, S. R. Parkin, *Org. Lett.* **2002**, *4*, 15–18.
- [51] B. D. Lindner, F. Paulus, H. Reiss, U. H. F. Bunz, unpublished results.
- [52] C. Wang, Z. Liang, Y. L. Liu, X. Wang, N. Zhao, Q. Miao, W. Hu, J. Xu, *J. Mater. Chem.* **2011**, *21*, 15201–15203.